Atmospheric Composition Change and its Climate Effect Studied by Chemical Transport Models

Project Representative

Hajime Akimoto Frontier Research Center for Global Change, Japan Agency for Marine-Earth Science and Technology

Authors

Prabir K. Patra *1, Kentaro Ishijima *1 and Takashi Maki *2

*1 Frontier Research Center for Global Change, Japan Agency for Marine-Earth Science and Technology

*2 Global Environment and Marine Department, Japan Meteorological Agency

We used two, NIES/FRCGC and JMA, chemistry-transport models (CTMs) and the CCSR/NIES/FRCGC atmospheric general circulation model (AGCM) based CTM (ACTM) in this project. ACTM is used to simulate atmospheric carbon dioxide (CO_2), sulphur hexafluoride (SF_6) for the period 1950-present. A model-data comparison of SF_6 is shown here for the period 1960–1998 and detailed analysis of trends in CO_2 seasonal cycle is being carried out. In the later part we discuss intercomparison of CO_2 fluxes derived by the 64-region time-dependent inverse (TDI) model of atmospheric-CO_2 based on the forward simulations using the JMA and NIES/FRCGC CTMs.

Keywords: greenhouse gases, transport modeling, source-sink inversion

1. Forward modeling of SF_6 and CO_2 during 1960–2005

The ACTM is nudged with ECMWF 40-year reanalysis (ERA40; period 1960–2002) and NCEP2 reanalysis (period: 2002–2006) for this work (ref. Patra et al., 2008 for details). There is a clear advantage of using computationally expensive ACTM for this simulation over the other less demanding CTMs that are driven by analyzed meteorology. This AGCM intrinsically generate detailed meteorology, e.g., advection, eddy mixing, convection consistently over the whole simulation period. The simulation results of SF_6 and CO_2 are analysed for the period since 1960. Since these gases are longlived in the troposphere and stratosphere (no chemical loss), a spin-up run for the gas concentration and model transport by running ACTM for the period 1950–1959.

For SF_6 concentration simulation, we have used SF_6 emission distributions from EDGAR (Olivier et al., 2001), and the global total emissions scaled based on the trends derived by Maiss et al (1996) for their analysis period of 1978–1995 and afterwards by the NOAA ESRL observed trends in atmospheric SF_6 concentration. Prior to 1978, the SF_6 emissions are extrapolated following a fitted curve to Maiss et al. (1996) measurements at Cape Grim (CGO). Using this SF_6 emission database and the nudged ATCM at T42 horizontal resolution, we are able to simulate the full evolution of SF_6 in the atmosphere (Fig. 1). SF_6 is used as a dielectric material since the mid-twentieth century, and its low atmospheric concentrations (~one-tenth of a pptv) were first measured by James Lovelock (1971) as an application of his newly developed electron capture detector (ECD) for measuring chemical compounds with high electron affinity. More regular observations are available since the 1970s (Maiss et al., 1996) and presently at tens of sites worldwide (e.g., Geller et al., 1997). The ACTM is also able to successfully simulate the synoptic variations, seasonal cycles and inter-hemispheric gradients when compared with observations at various time and space scales (see Patra et al, 2008 for further details).

The longest serving sites for atmospheric CO_2 concentrations are operated by the Scripps Institution of Oceanography

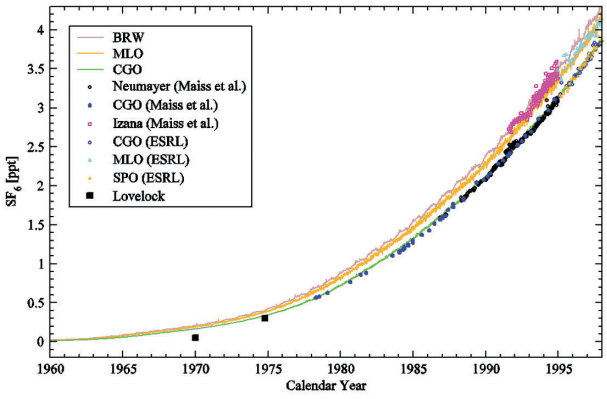

Fig. 1 Comparisons of simulated (lines) and observed (symbols) time series of SF_6 at several stations (see legends). The observation data are taken from three measurement programs (Lovelock et al., 1971; Maiss et al., 1996; Geller et al., 1997).

(SIO) at South Pole (SPO; 89.9˚S, 24.8˚W) and Mauna Loa (MLO; 19.5˚N, 155.6˚W) (Keeling et al., 2001; data available at http://scrippsco2.ucsd.edu). The ACTM modeled and observed CO_2 seasonal cycles are compared at 2 sites covering the whole simulation 1960–2005. We find that a significant part of the observed increases and recent decreases in CO_2 seasonal cycle are arising from the variabilities in atmospheric transport and seasonality in transport of fossil fuel emission.

2. Intercomparison of CO_2 fluxes derived by inverse modeling

This year, JMA group has adopted the 64-region division method by Patra et al., (2005) and simulated tracer transport with high resolution (1.0 × 1.0 degree in horizontal, much finer than NIES/FRCGC transport model of 2.5 × 2.5 degrees) CDTM with analyzed meteorological field. This number of region is one of the highest resolutions in current carbon-cycle research. We have estimated CO_2 monthly mean fluxes from 1991 to 2006 using time-dependent inversion (TDI) with two transport models (FRCGC and JMA). The 90 observational sites (Fig. 2) are selected from WMO/WDCGG (World Data Center for Greenhouse Gases) on the condition that the data selection rate by the inversion is larger than 50%.

Figure 3 shows the differences between the JMA and NIES/FRCGC CTM's transport. We have emitted 1 GtC/y CO_2 tracer from northern, tropical and southern areas in January 2000. These unit emissions are transported as tracer using both transport models (referred to response functions for each regional unitary emission). A comparison of the tracer concentration evolution at SPO is shown in Fig. 3. The northern and tropical tracer cases, FRCGC model tends to show higher concentrations than JMA model. However, JMA model shows higher concentrations at southern tracer case. This means that FRCGC model can transport remote tracer faster than JMA. These transport features affect surface flux estimation by TDI model from atmospheric data due to a particular forward transport model.

Figure 4 shows the intercomparion of CO_2 fluxes derived by TDI model using the regional response functions simulated by JMA and NIES/FRCFC forward models. We find that there are similar features in estimated CO_2 flux variability in

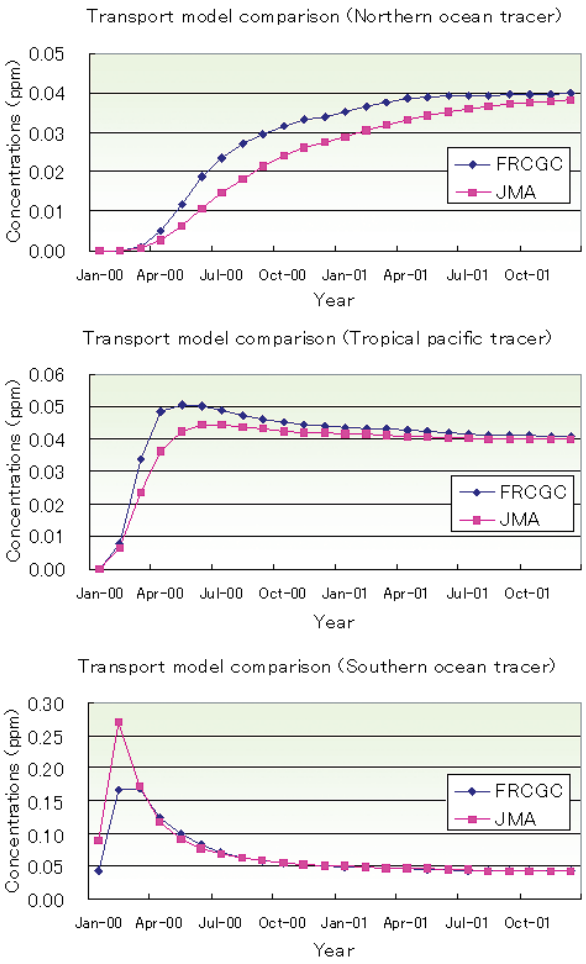

Fig. 3 Comparison of FRCGC and JMA forward model simulated tracer concentration evolution due to unitary regional source at South Pole (SPO).

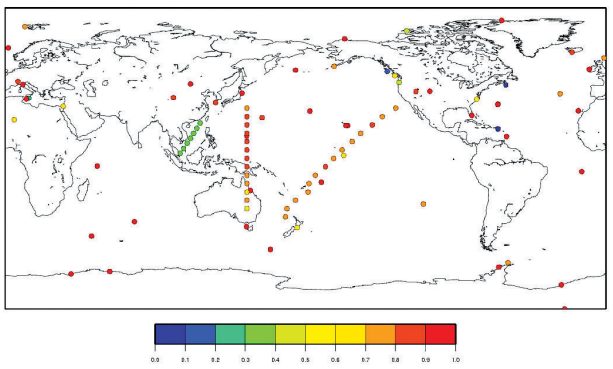

Fig. 2 The observational sites used in the inversion intercomparison. The colour bar shows the fractional data availability rate in the analysis period (full range: 0–1; interval: 0.1).

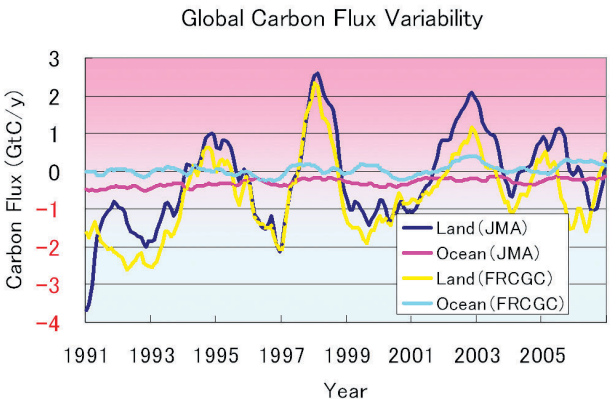

Fig. 4 CO_2 flux variability as estimated by time dependent inversion with FRCGC and JMA transport model. Twelve-monthly running means are taken to remove the seasonal cycle component from the estimated monthly flux time series.

global scale between FRCGC and JMA transport model. In regional scale, the estimated CO_2 fluxes show the similar phase and amplitude of CO_2 flux variability but there are some growing differences in less constrained land areas. These growing differences seem to come from the difference of model resolution and tracer transport scheme. The agreement between inverse model estimated CO_2 flux variability based on two different forward transport reiterates the fact that eventhough the absolute flux determination greatly depends in the forward transport model in use, the flux variability at interannual time scale can be derived realistically using single model transport.

References

Geller, L. S., J. W. Elkins, J. M. Lobert, A. D. Clarke, D. F. Hurst, J. H. Butler, R. C. Myers, Tropospheric SF_6: Observed latitudinal distribution and trends, derived emissions and interhemispheric exchange time, Geophys. Res. Lett., 24, 675–678, 1997.

Keeling, C. D., S. C. Piper, R. B. Bacastow, M. Wahlen, T. P. Whorf, M. Heimann, and H. A. Meijer, Exchanges of atmospheric CO_2 and $^{13}CO_2$ with the terrestrial biosphere and oceans from 1978 to 2000. I. Global aspects, SIO Reference Series, No.01–06, Scripps Institution of Oceanography, San Diego, 88 pp., 2001.

Lovelock, J. E., Atmospheric fluorine compounds as indicator of air movements, Nature, 230, 379, 1971.

Maiss, M., L. P. Steele, R. J. Francey, P. J. Fraser, R.L. Langenfelds, N.B.A. Trivett, and I. Levin, Sulfur hexafluoride: A powerful new atmospheric tracer, Atmos. Environ., 30, 1621–1629, 1996.

Olivier, J. G. J., and J. J. M. Berdowski, Global emissions sources and sinks, in The Climate System, edited by J. Berdowski, R. Guicherit, and B. J. Heij, A. A. Balkema Publishers/Swets & Zeitlinger Publishers, Lisse, The Netherlands, ISBN 9058092550, pp.33–78, 2001.

Patra, P. K., S. Maksyutov, M. Ishizawa, T. Nakazawa, T. Takahashi, J. Ukita, Interannual and decadal changes in the sea-air CO_2 flux from atmospheric CO_2 inverse modelling, Global Biogeochem. Cycles, 19, GB4013, 2005.

Patra, P. K., M. Takigawa, G. S. Dutton, K. Uhse, K. Ishijima, B. R. Lintner, K. Miyazaki, and J. W. Elkins, Transport mechanisms for synoptic, seasonal and interannual SF_6 variations in troposphere, Atmos. Chem. Phys. Discuss., submitted, 2008.

全球・地域スケール化学輸送モデルによる大気組成変動とその気候影響の研究

プロジェクト責任者
秋元　肇　海洋研究開発機構　地球環境フロンティア研究センター
著者
プラビール・パトラ*1，石島健太郎*1，真木　貴史*2
*1　海洋研究開発機構　地球環境フロンティア研究センター
*2　気象庁　地球環境・海洋部

1. SF_6とCO_2の長期シミュレーション

SF_6およびCO_2濃度について1950–2005年にかけて長期シミュレーションを行った。輸送場としてはERA40 (1960–2001年) とNCEP2 (2001–2005年) の再解析気象データを用いた。大気大循環モデルを用いたこのように長期間にわたる温室効果気体の計算を行った例はこれまでなく、温暖化を含めた様々な影響による温室効果気体の時空間変動の長期トレンドを調べる上で非常に有効な手段である。SF_6については観測濃度の季節変化や南北勾配など、様々な時空間スケールの変動を全計算期間にわたり良く再現した。CO_2濃度についてもマウナロア山や南極点における長期観測値と比較して良い結果が得られ、これまで論点となってきたそれら観測点におけるCO_2濃度の季節変化振幅の増減は大気輸送の長期変化によりほぼ説明されるということが分かった。

2. 逆計算により推定されたCO_2フラックスの相互比較

FRCGCとJMAのそれぞれの大気輸送モデルを用いて、逆計算により1991–2005年について推定されたCO_2フラックスを比較した。推定されたCO_2フラックスの全球的な時間変動に関して両者はほぼ同様の変動を示したが、地域ごとに比べると、解像度や輸送スキームに起因して陸域におけるフラックス値の相違が認められた。これから、推定されるフラックス値の空間分布については用いるモデルの輸送場に依存するが、フラックスの長期的時間変動に関しては一つのモデルで十分に推定可能であるということが分かった。

キーワード：温室効果気体, 大気輸送モデル, 放出源・吸収源の逆計算による推定